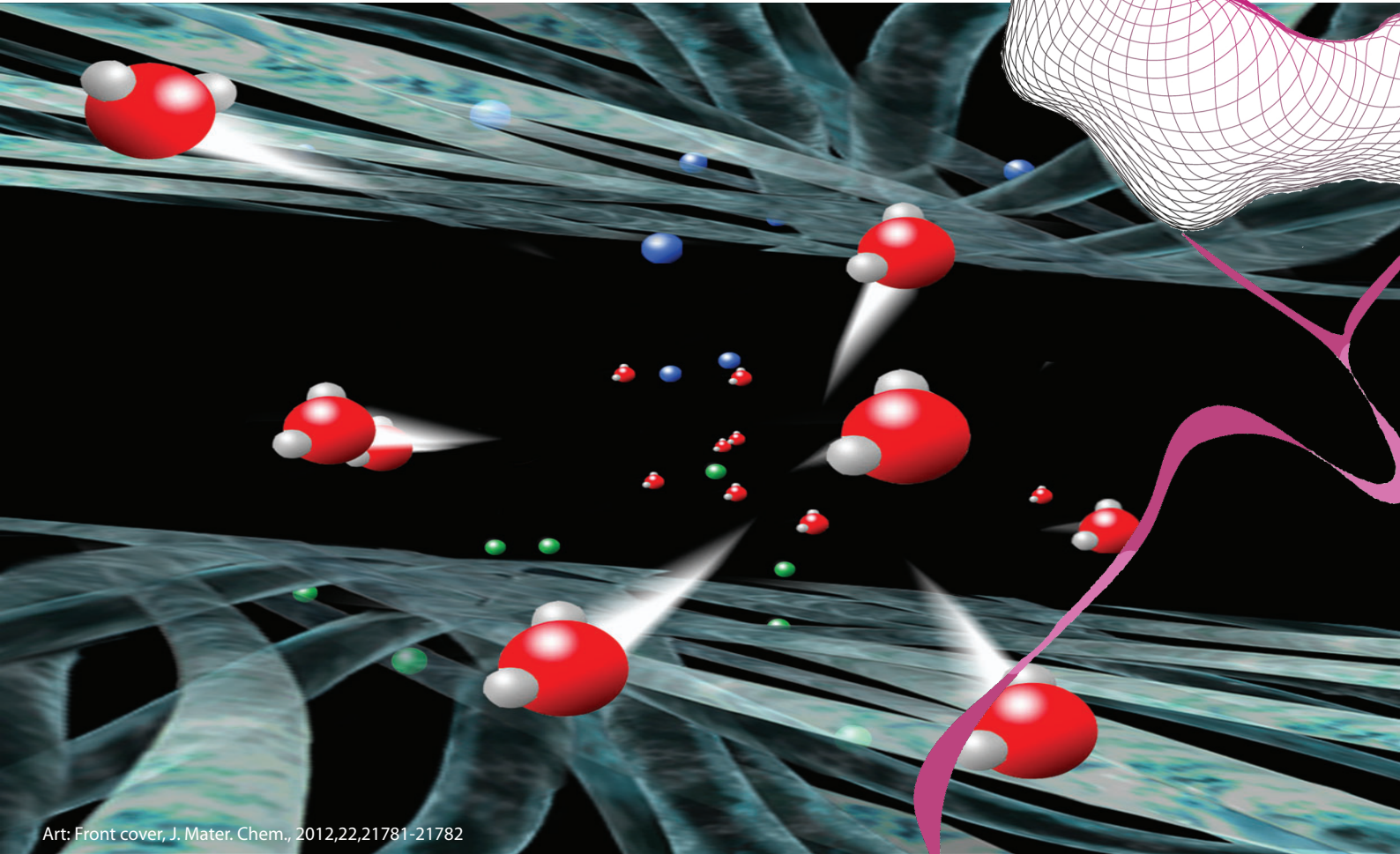


Characterization of capacitive deionization concentration profiles for small volume sample preparation.



Art: Front cover, J. Mater. Chem., 2012,22,21781-21782

Master thesis

M. J. van Rooijen

University of Twente, Electrical Engineering

Chair: BIOS Lab-on-a-Chip

Examination committee:

Prof.dr.ir. J.C.T. Eijkel (BIOS)

Dr. M. Odijk (BIOS)

S.H. Roelofs (BIOS)

Dr. J. R. T. Seddon (NI, TNW)

Time and date: 11h, 27 June 2014

Characterization of capacitive deionization concentration profiles for small volume sample-preparation.

Introduction

First, a small introduction will be given in what this master thesis has been about and how it developed over time. After this, the seemingly unusual format of this thesis will be explained. The overall goal of the project is to develop a microfluidic chip for the purpose of desalination of water. Two carbon electrodes are placed oppositely to each other with a liquid flowing in between. When a potential is applied over the electrodes the electric field will apply a force on the ions in the liquid. Negative ions will travel towards the positive electrode and vice versa. This leaves a deionized liquid behind.

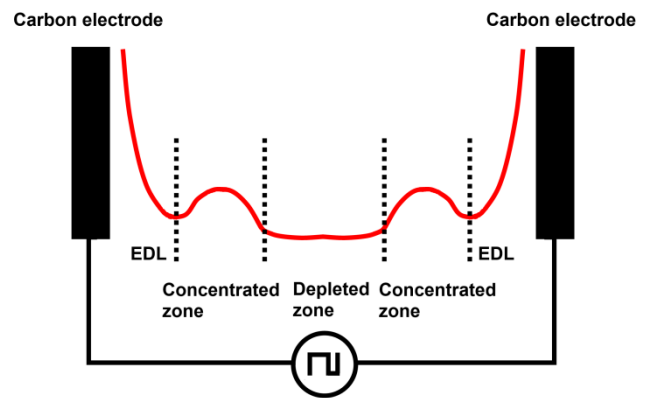


Figure 1 Schematic representation of the expected concentration profile by applying a square wave potential. Shown are the electric double layer and the concentrated and depleted zone.

Background

At the start of the project, it was believed that concentrated and depleted zones of ions would form when a square wave with a duty cycle $\neq \frac{1}{2}$ is applied to the electrodes. The reasoning behind this was that when a potential is applied ions are adsorbed to the electrode. After a short time, a balance exists between the migrational force and the diffusional force. However, when the potential is removed, the ion gradient will force the ions at the electrode back towards the middle of the channel. As electro neutrality has to hold for all positions except the electric double layer, it was believed that this movement would pull ions from the bulk towards the electrodes. This would result in an overlapping region just outside the diffuse layer where ions would accumulate. With a well-chosen frequency and duty cycle of the square wave, this effect could be maintained and a concentrated zone of ions would form.

The hypothesis was that these concentrated zones would indeed form. The goal was to first perform simulations to confirm the hypothesis and from there develop and fabricate a microfluidic chip that would incorporate this method of desalination. Ideally, the chip would be tested and the simulation findings would be confirmed.

In practice, the simulations did not show the ion profile we expected and is shown in the figure. The simulations did show that capacitive deionization is a localized process. When a potential is applied, the flux of ions towards the electrodes come from the region just beyond the diffuse layer. The concentration in this region is thus lower than in the bulk. After some time, the ions in the bulk move towards this depleted zone, equalizing the charge distribution.

From these findings the project was shifted towards determining if these findings for the simulations were correct. Therefore, a setup was designed and fabricated to confirm these simulations.

Outline

Instead of the normal report form that have been the standard for some time, it is now also allowed to write the master thesis in a paper like format. Because this seemed like a good opportunity to get some education in academic writing, I have written a paper for the fictional magazine *BIOS Lab on a Chip* published by UTPublishing (University of Twente Publishing). As this is the first volume, the magazine still has to find its identity.

The paper will be the basis of the report on the project. As a paper is limited in size, it will be accompanied by supplementary info (SI). Although effort has been made to create a paper that is worth publishing, it must be noted that more testing is necessary. The results have to be reproduced and some details need clearing up. In my belief, this should make the results and more importantly the conclusions a lot stronger.

The paper and supplementary info will be followed by the acknowledgements.

ARTICLE

Characterization of capacitive deionization concentration profiles for small volume sample-preparation.

Cite this: DOI: 10.1039/x0xx00000x

Received 30th May 2014,
Accepted 27th June 2014

DOI: 10.1039/x0xx00000x

www.rsc.org/

M.J. van Rooijen,^a S.H. Roelofs,^a A van den Berg,^a J.C.T. Eijkel,^a and M. Odijk^a

Capacitive deionization (CDI) is an upcoming method for desalination of aqueous solutions. With its low energy consumption and low-pressure operation, it shows promise in general, but also as a method for small volume sample pre-treatment. A lot of sample pre-treatment for lab on a chip (LOC) devices is still done off chip. To integrate CDI as a continuous method into a LOC, research has been performed to understand the distribution of ions during CDI. A one-dimensional computational model has been constructed to simulate mass-transport over time during CDI. Next, a neuroprobe was used to determine the impedance (EIS) at different positions between two porous carbon electrodes (3.1mm separation). The simulations show that CDI is a localized process, which is confirmed by the measurements. It shows that the highest amount of deionization takes place just beyond the Debye length and declines towards the centre. Due to the non-homogenous distribution of the ions, it seems CDI can be used as a continuous method of deionization under flow conditions.

Introduction

There has been a steady increase in the consumption of clean water. This is accompanied by higher demands on the allowed solutes in the water. This is why research is focussing on finding novel ways to deionize water and ways to improve existing methods. The main focus is increasing efficiency and reducing costs. The latter by reducing energy consumption and improving the durability of the used materials.¹

Common methods for deionization are reverse osmosis (RO), multistage flash distillation (MSF) and multi effect distillation (MED) which were responsible for 94% of the capacity of deionization installations in 2012.¹

One of the upcoming methods is capacitive deionization (CDI). Research into CDI has started in the late 1960s making it a relatively young field of research.^{2,3} Some clear advantages are seen for this technology like low-pressure operation, which reduces cost. A low voltage reduces safety issues and lowers energy consumption, which could make it a possible candidate to be supplied by solar energy. It would also make it a good candidate for lab on a chip devices (LOC). Especially as a method for small sample pre-treatment.^{4,5} It could for instance be used to prepare samples for liquid chromatography (LC) and mass spectrometry (MS).^{6–8}

The concept of CDI is based on a pair of porous electrodes over which a voltage is applied. Due to the electric field, the ions in the solution will migrate to their respective oppositely charged electrodes. The ions will be adsorbed to the electrodes, leaving a deionized solution behind. This is depicted in Figure 1. When the deionized solution is flushed out, the electrodes can be short-circuited or a reversed potential can be applied such that the ions will be released into the currently available solution. In general, this is the same starting solution and in the end, there will be a deionised solution and a solution with increased ion levels.

There are several ways this concept has been implemented. Some differ in the way the electrodes are positioned with respect to the flow of solution, others differ in the way the solution is controlled in respect to the adsorption and desorption phase of the CDI process.

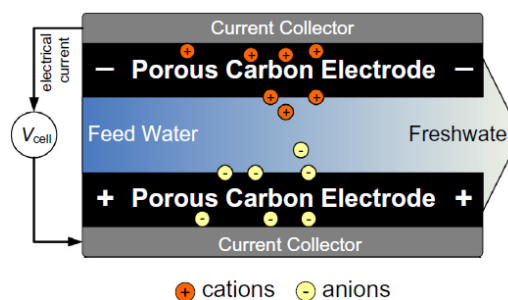


Figure 1 Schematic representation of the workings of CDI. A voltage is applied over two porous carbon electrodes resulting in ions moving from and to the electrodes. The result is fresh water leaving the channel. Reprinted with permission from S. Porada et al.²

Three relevant CDI geometries are the flow-by mode, the flow-through mode and electrostatic ion pumping which are shown in Figure 2.² With the flow-by mode the electrodes are positioned parallel to the flow. The applied electric field will therefore be perpendicular to the flow as will the migration of the ions.

In the flow-through mode, the electrodes are positioned perpendicular to the flow, meaning the solution passes through the electrodes. When a potential is applied between the electrodes the ions stay behind at the surface of the electrodes. A special case of these two modes is desalination with electrode wires seen in Figure 2D.^{2,9} In this case the solution does not pass through the electrodes, but the solution passes the electrodes that stand in the flow of the solution.

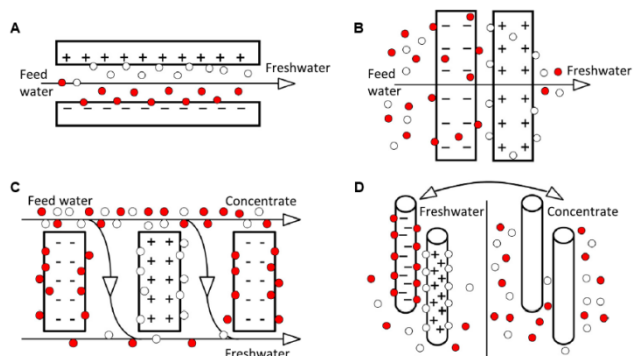


Figure 2 Four CDI geometries. A: flow-by mode. B: Flow-through mode. C: Electrostatic ion pumping. D: Electrode wires positioned in the flow of the solution. Reprinted with permission from S. Porada et al.²

With electrostatic ion pumping two supply channels are positioned parallel to each other, connected to each other by parallel channels which are perpendicular to these two supply channels (Figure 2C).¹⁰ The channels connecting the two supply channels are separated by electrodes. By controlling the flow in the two supply channels, the flow and the direction of the flow between the two channels can be controlled. By synchronizing the potential applied to the electrodes with the movement of the fluid in between the two supply channels, ions can be adsorbed when the fluid flows one way, and desorbed when it flows the other way. This results in one channel containing a low ion concentration while the other will have an increased ion concentration.

Because of the concept of CDI, these modes have in common that they rely on the electrodes to adsorb large amounts of ions. This is why a lot of research is focussing on improving the capacity of the electrodes. This is partially achieved by exploring different forms of porous carbon and to lesser extent other materials. Another way is to put membranes in front of the electrodes.^{2,11–15} All modes previously mentioned have been tried both with as well as without membranes and with different types of porous electrodes.^{2,3,16,17} Parallel to this research of materials for the benefit of CDI, theoretical research is employed to understand the interaction of ions with the porous materials and membranes. A particular interest goes out to the understanding of the different sizes and arrangement of pores in these porous materials. Although the focus on materials can be explained by increasing the capacity and therefore the efficiency, it can also be explained by the need for the materials to be mechanically stable for longer periods of time and being able to withstand fouling.^{1,18}

As mentioned, CDI can be used as a pre-treatment tool for input samples of LOC devices. A lot of research is done miniaturizing analysis methods. However, the miniaturization of sample pre-treatment lacks behind and is still mainly done beforehand in the lab.^{4,19} This is fine for research and analysis in labs, but with the rising technologies of point-of-care systems, this cannot be expected to be done by the end-user. Examples of analysis methods that benefit from deionization as a sample pre-treatment method are LC and MS.^{6–8}

CDI seems to have the benefits of being operated at low pressures and at low energy consumption in contrast to other methods of deionization. Because of these features and the fact that it can be scaled down in size, makes it a good candidate for deionization of small samples. Especially when it is integrated as a pre-treatment method in a LOC device. Mainly because pre-treatment is commonly still done outside of the LOC device. The question arises how CDI can be used as a sample pre-treatment method. Especially when a continuous flow of deionized solution is needed. There is a lot of information available on the efficiency of CDI in literature. However, there is not much information on how the ions are distributed during deionization. The majority of research focusses on how many

ions are adsorbed or what the concentration is of the (total) output flow. We think it is necessary to know the distribution of ions to create a continuous deionization method for small sample pre-treatment. Therefore, we have conducted simulations and measurements to provide details on ion concentrations during deionization. The simulations will show that deionization is a localised process. Via measurements of the concentration at different locations, we try to confirm these simulation results.

Theory

Simulation of desalination between two planar electrodes when applying a potential.

For a first impression of desalination using two planar electrodes, a simulation has been performed using COMSOL Multiphysics 4.4. To keep the model simple, the two planar electrodes with the NaCl solution in between, has been simulated in a one-dimensional model. The boundaries representing the electrodes are spaced 3.1mm from each other. The electrolyte is composed of 0.02mol/m³ NaCl dissolved in water. This concentration is chosen to compensate for the carbon electrodes being porous. It is estimated that the porous nature of the carbon electrodes increases the surface area by a factor thousand.^{20–22} This is relative to an ideal smooth surface, which is assumed in the model. The definition of concentration is the total amount of ions in a certain volume. The area the ions ‘see’ towards the electrode is a thousand times bigger than with a smooth surface. The difference in area could therefore be approximated by decreasing the concentration by the same factor. This seems justifiable, because the applied potential is the same for the total surface area of the carbon. Simulating with 0.02mol/m³ would therefore be comparable by a real situation of carbon electrodes and a 20mol/m³ solution.

It must be noted that this is an oversimplification of modelling porous carbon electrodes. It for instance does not take into account the dynamics introduced by the different pore sizes. To keep the model simple this method was preferred at this stage.

The self-ionization of water is not included in the model, meaning that the only electrochemically active species are the sodium and chloride ions. Because of their similarities in size and charge, the mobilities of the sodium and chloride are equal. In the model they are assumed equal, resulting in a symmetric system (see Table 1).

The flux of ions is simulated using the Nernst-Planck equation:

$$J_j(x) = -D_j \frac{\partial C_j(x)}{\partial x} - \frac{z_j F}{RT} D_j C_j \frac{\partial \phi(x)}{\partial x} + C_j \vec{v}(x) \quad \text{Eq. 1}$$

Where:

- J_j = Flux of ion species j [mol·m⁻²·s⁻¹]
- D_j = Diffusion coefficient of ion species j [m²·s⁻¹]
- C_j = Concentration of ion species j [mol·m⁻³]
- z_j = Valence of ion species j
- ϕ = Electric potential [V]
- \vec{v} = Velocity of the surrounding fluid (0) [m·s⁻¹]
- F = Faraday constant (96485) [C·mol⁻¹]
- R = Gas constant (8.314) [J·mol⁻¹·K⁻¹]
- T = Temperature (298) [K]

The three terms on the right of Eq. 1 represent the respective contributions of diffusion, migration and convection to the flux. In the simulation the convection contribution is set to zero ($v=0\text{m}\cdot\text{s}^{-1}$), so only the effects of diffusion and migration are studied.

For the electric potential profile, the Poisson-Boltzmann equation is used:

$$\frac{\partial^2 \phi(x)}{\partial x^2} = -\frac{\rho}{\epsilon_0 \epsilon_r} = -\frac{F}{\epsilon_0 \epsilon_r} \sum_j z_j \cdot C_j \quad \text{Eq. 2}$$

Where:

$$\begin{aligned} \rho &= \text{Charge density per unit volume [C}\cdot\text{m}^{-3}] \\ \epsilon_0 \cdot \epsilon_r &= \text{Dielectric permittivity (6.9061E-10) [F}\cdot\text{m}^{-1}] \end{aligned}$$

The Poisson-Boltzmann equation includes the formation of a diffuse layer as proposed in the Gouy-Chapman theory for the double layer but it does not compensate for the finite size of the ions near the surface of the electrode as proposed by the Stern modification to the Gouy-Chapman theory²³. To incorporate this modification without increasing the computation time of the simulation, this modification is included in the boundary conditions. This means that the boundaries of the simulation model, are located at the closest the ion centres can approach the electrode surface (the outer-Helmholtz or Stern plane). Because the charge density in between the electrode and this layer is zero, the electric field strength is constant over this Stern plane. This means the potential drop over this Stern plane will be linear²³. The resulting boundary equation is:

$$\frac{\partial \phi(x)}{\partial x} = \frac{\phi_{el} - \phi(x)}{\lambda_s} \quad \text{Eq. 3}$$

Where:

$$\begin{aligned} \phi_{el} &= \text{Electric potential applied over the electrodes} \\ &\quad (0.75) \text{ [V]} \\ \lambda_s &= \text{Distance between the electrode and the Stern layer} \\ &\quad (3\text{e-}10) \text{ [m]} \end{aligned}$$

Between the electrodes, a potential difference of 0.75V is applied for 15 minutes. After this period, the electrodes are short-circuited for the following 15 minutes.

Table 1 Constants for the Na⁺ and Cl⁻ ions. Their mobilities are calculated using the Einstein-Smoluchowski relation.

Constant	Value
C_{na}	0.02
C_{cl}	0.02
D_{na}	2e-9
D_{cl}	2e-9
μ_{na}	$\frac{D_{na} \cdot F}{R \cdot T} = 7.7887\text{e-}8$
μ_{cl}	$\frac{D_{cl} \cdot F}{R \cdot T} = 7.7887\text{e-}8$
Z_{na}	+1
Z_{cl}	-1

For more details on the model and the used settings, see SI-1.

Experiments

A desalination cell has been created by clamping two carbon sheets between two 4x4cm PMMA plates. A U-shaped PDMS spacer is used to separate the carbon sheets (contribution Voltea B.V., Sassenheim, The Netherlands) and create a fluid compartment. This can be seen in Figure 3A and D. In Figure 3A the PDMS spacer is portrayed in yellow. The dashed blue line marks the fluid compartment. The compartment is $\sim 2 \times 1\text{cm}$ and has a spacing of 3.1mm. Before this cell is put together, the carbon sheets are pre-soaked for 24h before measurements in 20mM NaCl solution (Sigma-Aldrich). This 20mM NaCl solution is the same as the liquid used for desalination. This is done to increase the reproducibility of the measurements, as it seems to cost time for the carbon to be wetted.

A sensor is inserted into the liquid, which is connected via a metal L-shape to a micropositioning table (Figure 3). By adjusting the table, the sensor can be accurately repositioned between the two carbon electrodes with a maximum resolution of $20\mu\text{m}$ over a range of 1.5cm.

The sensor is a small neuroprobe with a shaft diameter of $160 \times 160\mu\text{m}$.²⁴ The tip consists of multiple electrodes from which two electrodes (E1 and E2) are used to perform electrochemical impedance spectroscopy (EIS) measurements. The whole sensor and probe tip can be seen in Figure 3B and C. The electrodes are spaced $63\mu\text{m}$ apart from centre to centre and have a diameter of $50\mu\text{m}$. The electrodes are recessed for $5\mu\text{m}$. The carbon electrodes are connected to a buffered, battery powered, DC voltage source of 0.75V. Because the power source is battery powered it prevents grounding issues.

A switch controls whether this potential is applied or if the electrodes are shorted. A simplified schematic can be seen in Figure 4A and a more detailed schematic can be seen in SI-2.

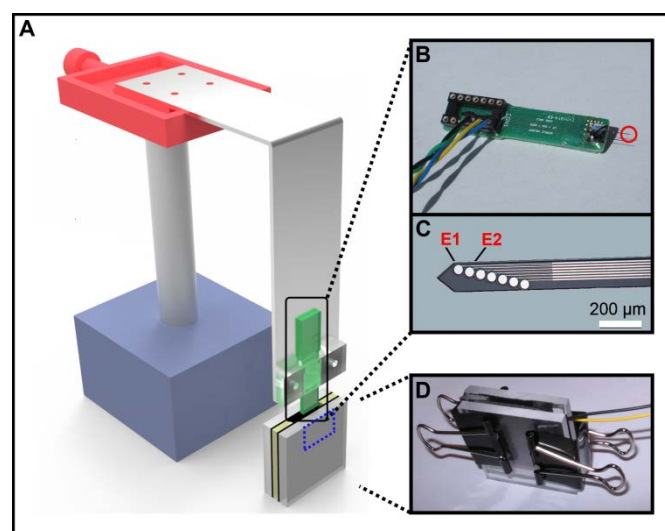


Figure 3A: Schematic overview of the measurement setup. The blue dashed line represents the volume ($\sim 2 \times 1\text{cm}$) of the deionization cell. In red the micropositioning table. In green the sensor, which is enlarged in B. The red highlight is the tip of the neuroprobe that can be seen in C with the electrodes E1 and E2 ($50\mu\text{m}$ diameter). D shows the deionization cell with from top to bottom: PMMA plate, carbon sheet, U-shaped PDMS spacer (yellow), carbon sheet and PMMA plate.

The EIS measurement is done at a fixed frequency by connecting the sensor electrodes to an in-house developed lock-in amplifier. The lock-in amplifier is 14-bit and DSP based. A schematic representation of the lock-in amplifier can be seen in Figure 4B.

An AC potential of $0.15V_{rms}$ at a frequency of 35kHz is applied over the sensor electrodes in series with an $81.5k\Omega$ resistor. The resulting response is measured over the sensor leads (see Figure 4B), with a sample frequency of 400kHz, which results in 476.84Hz after decimation.

Measurements take place for different positions between the two carbon plates, where the step size, Δx , is smaller near the electrodes, while it increases near the centre. The $0.75V$ is applied for 15min, which is followed by 15min of the carbon electrodes being shorted. During these 30min of time, the impedance is measured using the sensor electrodes. Afterwards the sensor is repositioned using the micropositioning table and the process is repeated.

The whole setup is placed in a Faraday cage except for the lock-in amplifier. Large openings in the cage are sealed to reduce airflow. The humidity inside the cage was increased by adding a water container with large area opening inside the cage. This is to reduce the effects of evaporation and convection on the measurement.

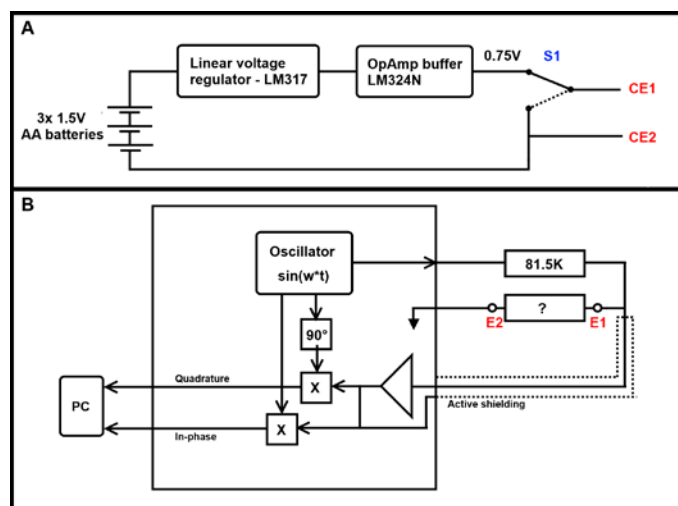


Figure 4A: Battery powered DC voltage source connected via a switch (S1) to the carbon electrodes CE1 and CE2. B: Schematic overview of the EIS measurement. The oscillator output connected via a shunt resistor to the neuroprobe electrodes (E1 and E2). The impedance measured via a buffer over the electrodes. The measurement wire is actively shielded.

Results

Simulation

The conductivity is proportional to the sum of the concentration of all electrochemically active ions. The simulation results will be shown as the sum of the concentration of the Na^+ and Cl^- ions. This way it is possible to compare the simulation results with the EIS measurements later on. To increase the readability of the graph, the bulk concentration of both ion species is subtracted. Therefore, positive values will show an increase of ions relative to the bulk concentration and negative values will show a decline of ions relative to the bulk concentration.

In Figure 5, the results are shown for the simulation. Figure 5A shows the relative concentration over the total distance between the electrodes. This is the concentration profile 10s after the potential is applied over the electrodes. The concentration of ions has a sharp increase close to the electrode. Please note the discontinuous y-axes. At 10s, the peak will reach $2431mol/m^3$ at the electrode.

Besides the sharp increase in concentration, an area close to the electrodes up to $\sim 500\mu m$ from the electrodes shows a decline in concentration relative to the bulk. In the centre, the concentration stays at the bulk concentration.

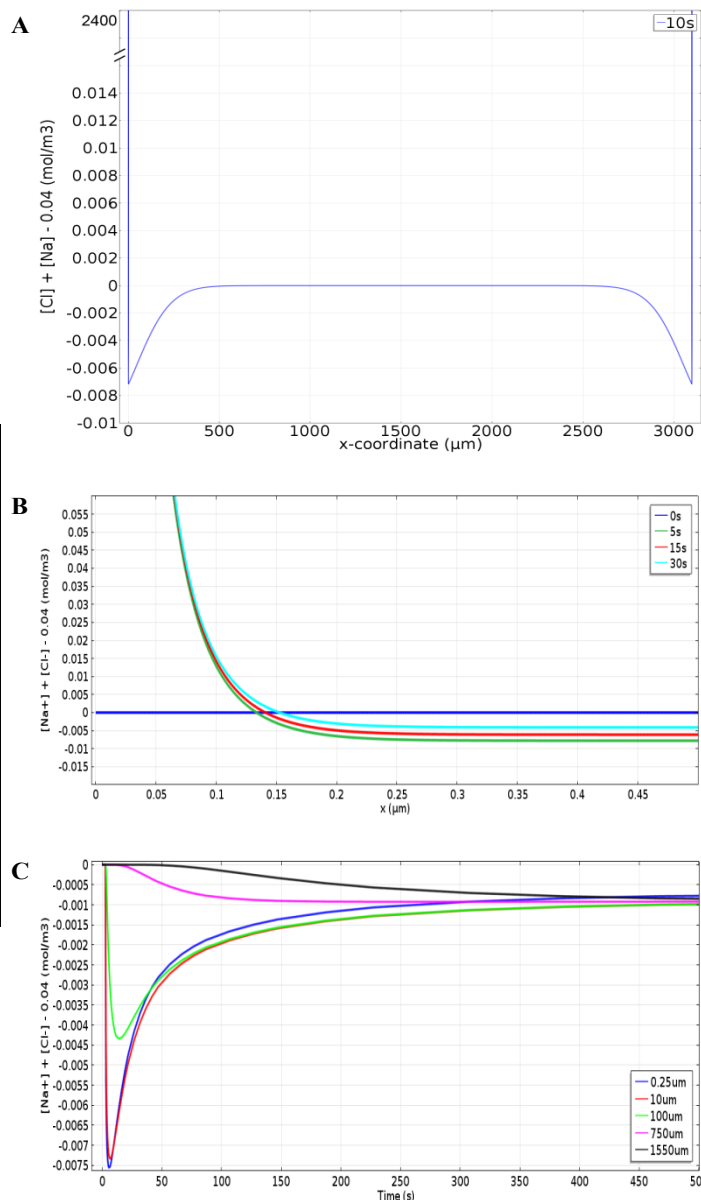


Figure 5 Simulation results where the sum of the Na^+ and Cl^- ions is shown relative to their initial concentration ($2 \cdot 0.02mol/m^3$). A: Concentration profile between the two electrodes 10s after applying a potential over the electrodes (note the discontinuous y-axes). B: The concentration profile at different times. The graph is zoomed in at the Debye length. C: The concentration over time at different positions between the electrodes ($1550\mu m$ is the centre).

Figure 5A also shows that the results are symmetrical. Due to the same mobility of the ions, this is expected. What the graph does not show is the contributions of the two ion species to the concentration. Although the summed concentration is

symmetrical, the concentration of the individual ion species is not. At the positive electrode, the concentration Cl^- will increase sharply, while the concentration Na^+ will fall to zero. At the negative electrode, the opposite happens.

Figure 5B shows the same graph only zoomed in to one of the electrodes. From the figure, it is concluded that the diffuse layer extends to about $0.15\mu\text{m}$. This distance is also called the Debye length. Beyond the Debye length, it can be seen that deionization takes place relative to the original concentration. Over time, the amount of deionization decreases.

In Figure 5C, the concentration has been plotted versus time for several positions between the electrodes. The first position is just after the Debye length, while the last one is at the middle between the two electrodes. Nearest to the Debye length, the amount of deionization is the highest in the first 10s and almost zero towards the centre between the electrodes. After an initial

peak, the amount of deionisation starts to decrease, while the amount of deionization towards the middle starts to increase. After approximately 400s, the amount of deionization starts to level out over the whole area beyond the Debye length.

When the combination of Figure 5A, B and C is considered, it seems likely that initially CDI is a localised process. This can be explained by the rapid movement of ions towards the electrode due to migration. Besides that, the rapid decline to zero of the concentration of the oppositely charged ion species. This results in an overshoot of deionization just beyond the Debye length, because electro neutrality has to apply everywhere. The concentration gradient that this causes will result in ions diffusing from the centre between the electrodes. From Figure 5C, it can be concluded that this process takes time.

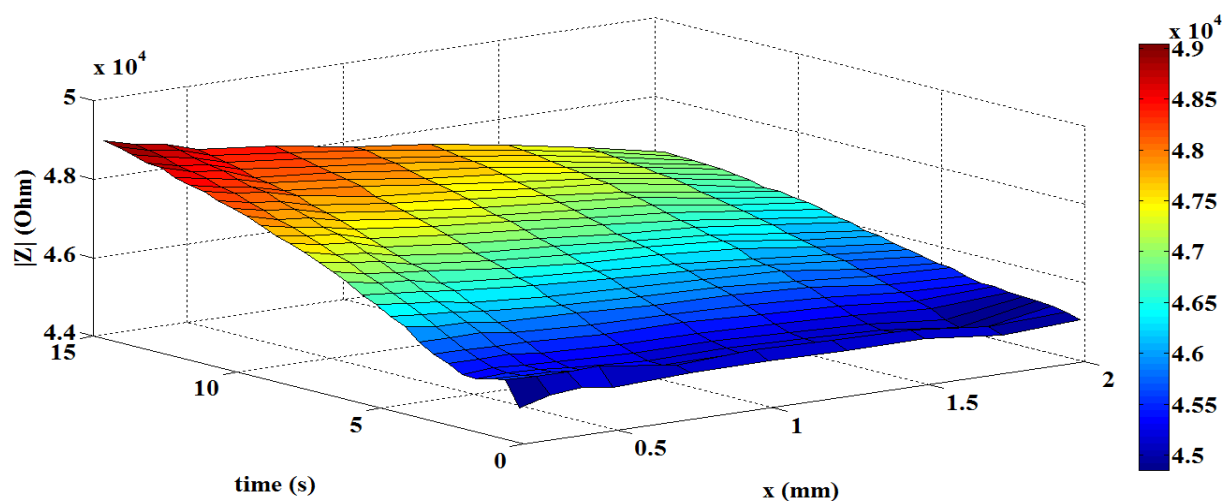


Figure 6 The impedance results are shown plotted against the distance and the time. An increase in impedance is consistent with a decrease in concentration of ions. The first measurement is performed with the neuroprobe near one of the carbon electrodes ($x=0\text{mm}$), but results are only shown from $x=0.20\text{mm}$ and further.

EIS measurements

Figure 6 shows a three-dimensional plot where the impedance is plotted against the time and the location. The impedance is the result of the EIS measurement with the neuroprobe. The location is the position of the neuroprobe between the two carbon electrodes. The first position of the neuroprobe was nearly zero with respect to one of the electrodes, but the precise distance could not be determined. The main reason for this is that the carbon sheets are not perfectly flat. This first position is defined as $x=0$ in Figure 6.

The plane of the electrodes of the probe was parallel to the carbon electrodes. At its first position the electrodes of the probes were facing the carbon electrode it was close to.

As can be seen in the graph the first position starts at 0.20mm . At the positions of the probe between 0mm and 0.20mm , it is believed that the close proximity of the probe influenced the measurement. At this distance, the cell constant is different from when the probe is further away from the carbon electrode. Therefore, it is impossible to compare the two situations without knowing how the cell

constant differs. Furthermore, at this distance the physical size of the neuroprobe is also of influence on the movement of the ions. This will therefore also influence the results of the EIS measurements.

The EIS measurement starts before the voltage is applied to the carbon electrodes. Figure 6 shows the impedance from the moment the voltage is applied to the carbon electrodes. First, a small rise of the impedance can be observed followed by a dip. After the dip, the impedance steadily rises over time. The dip is most likely explained by the sudden application of the potential. As the EIS measurement is already in progress, the electric field of the potential over the carbon electrodes distorts the measurement and rearranges the migrational flux of the ions.

The steady rise of the impedance is consistent with the expectation that the net movement of ions is towards the carbon electrodes. This leaves a lower concentration of ions at the measurement location. This in turn results in a lower conductivity and thus a higher impedance.

In Figure 6 it is clearly seen that closer to the carbon electrode the deionization takes place at a faster rate than at the centre between the two electrodes ($x\approx 1.55\text{mm}$). It can

also be concluded that the amount of deionization is even more prominent up to 0.5mm. This supports the idea that CDI is a localised process.

Finally, the conversion from impedance to concentration has to be considered. Measurements were done at a fixed frequency. The frequency was chosen by making a Bode-plot of a 20mM NaCl solution. From the Bode-plot, the frequency of the resistive plateau was determined. When the concentration however changes, the measurement is not done anymore at the resistive plateau. Therefore, the resistivity is in this case not linearly dependent on the concentration. The increase in impedance will be lower than the decrease in concentration. This is discussed in more detail in SI-3 with supporting graphs.

Due to the non-linearity between the impedance and the concentration, the decline in concentration is to a bigger extent in Figure 6. This makes the difference between the concentration close to the electrode and towards the centre even larger.

Comparison of the simulation to the EIS measurements.

Both the simulation and the EIS measurements show that the amount of deionization closer to the carbon electrode is higher than towards the centre.

However, the region to which it extends is much larger with the measurements in respect to the simulations. This could be due to the simplifications made in the model. It could be that the porosity of the carbon electrodes influences the extent of the diffuse layer. While the Debye length is increased due to the choice for concentration in the model, it is possible that the Debye length in reality is even bigger. This is however hard to predict without more measuring points closer to the carbon electrodes.

With the simulations, it was seen that the deionization levelled out at approximately 400s. This is not seen in the EIS measurements. It is not fully understood why this does not happen. It could be that the capacity to store ions of the carbon electrodes is so high that depletion still takes place near the Debye length. This at a higher rate than diffusion can transport ions to compensate.

As mentioned with the simulation it is expected to see symmetric results around the middle position ($x \approx 1.55\text{mm}$). This is because of the same size carbon electrodes and the use of a salt with ions that have the same mobility. This is not clearly seen in Figure 6. It seems that this can, at least partially, be explained by evaporation. However, more research is necessary to determine to what extent evaporation is the cause.

Due to the total time of the experiments, some evaporation takes place. This means the concentration of the ions will increase and therefore the impedance will decline. Furthermore, the waterline drops, so the area of the carbon electrodes that is in contact with the solution also decreases.

Overall, the EIS measurements seem to be consistent with the simulations in the sense that both show CDI is a localized process. Although a more complex model for simulation is needed to confirm the differences regarding the areas of deionization. This model should include the porous nature of the electrodes and more specifically the movement of ions near the surface and the resistances the ions need to overcome to reach the surface inside the electrodes.

It would also help to confirm the findings when measurements could be performed closer to the carbon electrode. With the current setup, this could be done by turning the neuroprobe 90 degrees. This way the dimensions of the probe will be of less influence on the ion movement. Most importantly, the cell constant should be approximately the same as when measurements are done positioned further away of the carbon electrodes.

Conclusions and outlook

Although the field of research into CDI is still very young, it is considered a promising technique. Especially its low power consumption and operation at low pressures let it stand out from other deionization methods. Besides this, it can be scaled down and therefore could be used as a method that integrates well into LOC devices.

Our simulations have shown that when two electrodes are separated 3.1mm apart, deionization takes place. More importantly, it also indicates that CDI is a localised process that takes place near the electrodes.

We have tried to reproduce these findings by measuring the concentration at different positions during CDI. The results show that the measurements are in line with the simulations. The results corroborate the idea that CDI is a localised process. However, the results show some inconsistencies most likely caused by evaporation due to the long duration of the experiments. For instance, symmetry is expected around the centre between the carbon electrodes. This is because of the equal mobilities of the sodium and chloride ions. The symmetry however was not seen in the measurements. More research should be conducted to have more knowledge on the impact of evaporation on the measurements.

Due to the setup limitations, it was not possible to show where the maximum deionization takes place. From the simulations, it was seen that the region with the highest deionization was just beyond the Debye length. Deionization declined towards the centre. With a different setup as discussed in the results section, measurements could be performed closer to the carbon electrodes. This should give an even better comparison to the simulations.

As stated in the introduction, the majority of research on CDI concentrates on its efficiency. This is mainly done by measuring how many ions are adsorbed or by measuring the concentration of the output solution. This has contributed to CDI setups that are discontinuous in nature. Most setups have a period where deionization takes place and a period where ions are released. This results in an output phase with a low and one with a high ion concentration. With the results presented in this paper, this could be done differently.

When a flow-by geometry is taken as seen in Figure 2A, we now know that the concentration of the output is not uniformly distributed. With this knowledge, it should be possible to compartmentalize the output. Without splitting the output, it also consists of the solution in the centre, which is still at the bulk concentration. By splitting the output, it is possible to have an output at a lower concentration ions. This at the cost of output volume.

It is furthermore hypothesized that a well-chosen square wave potential applied over the carbon electrodes will allow the deionization to be continuous. It is believed that when adsorption and desorption are cycled with the right timing, the region just beyond the Debye length will stay deionized. In combination with splitting the output, this would allow for continuous deionization.

Besides deionization as a goal, this method could also be used for other purposes. It could for instance create a

concentration gradient. This could for instance be interesting, when the influence of a substance gradient on a cell is researched. The substance could for instance be a toxic or nutrient for the cell. It is likely that with this method also a pH gradient can be created.

Acknowledgements

We like to thank Voltea B.V. for contributing the carbon electrode material.

Notes and references

^a Mesa+ Institute for Nanotechnology, University of Twente, THE NETHERLANDS.

Electronic Supplementary Information (ESI) available:

SI-1 Details of the one-dimensional Comsol model for capacitive deionization.

SI-2 Schematic of the battery powered voltage source.

SI-3 Overview EIS measurements for different ion concentrations.

See DOI: 10.1039/b000000x/

- 1 N. Ghaffour, T. M. Missimer, and G. L. Amy, *Desalination*, 2013, **309**, 197–207.
- 2 S. Porada, R. Zhao, A. van der Wal, V. Presser, and P. M. Biesheuvel, *Prog. Mater. Sci.*, 2013, **58**, 1388–1442.
- 3 Y. Oren, *Desalination*, 2008, **228**, 10–29.
- 4 A. J. de Mello and N. Beard, *Lab Chip*, 2003, **3**, 11N.
- 5 S.-M. Jung, J.-H. Choi, and J.-H. Kim, *Sep. Purif. Technol.*, 2012, **98**, 31–35.
- 6 B. L. Karger, D. P. Kirby, P. Vouros, R. L. Foltz, and B. Hidy, *Anal. Chem.*, 1979, **51**, 2324–2328.
- 7 S. Riediker and R. H. Stadler, *J. Chromatogr. A*, 2003, **1020**, 121–130.
- 8 F. Gharahdaghi, C. R. Weinberg, D. A. Meagher, B. S. Imai, and S. M. Mische, *Electrophoresis*, 1999, **20**, 601–5.
- 9 S. Porada, B. B. Sales, H. V. M. Hamelers, and P. M. Biesheuvel, *J. Phys. Chem. Lett.*, 2012, **3**, 1613–1618.
- 10 W. L. . Bourcier, R. D. . Aines, J. J. . Haslam, C. M. . Schaldach, K. C. . O'Brien, and E. Cussler, 2011, 10.
- 11 L. Alvarado and A. Chen, *Electrochim. Acta*, 2014, **132**, 583–597.
- 12 F. A. AlMarzooqi, A. A. Al Ghaferi, I. Saadat, and N. Hilal, *Desalination*, 2014, **342**, 3–15.
- 13 Ö. Arar, Ü. Yüksel, N. Kabay, and M. Yüksel, *Desalination*, 2014, **342**, 16–22.
- 14 Y.-J. Kim, J.-H. Kim, and J.-H. Choi, *J. Memb. Sci.*, 2013, **429**, 52–57.
- 15 P. M. Biesheuvel and A. van der Wal, *J. Memb. Sci.*, 2010, **346**, 256–262.
- 16 Y. Wimalasiri and L. Zou, *Carbon N. Y.*, 2013, **59**, 464–471.
- 17 H. Li, L. Pan, T. Lu, Y. Zhan, C. Nie, and Z. Sun, *J. Electroanal. Chem.*, 2011, **653**, 40–44.
- 18 M. a. Anderson, A. L. Cudero, and J. Palma, *Electrochim. Acta*, 2010, **55**, 3845–3856.
- 19 J. Lichtenberg, *Talanta*, 2002, **56**, 233–266.
- 20 A. Soffer and M. Folman, *J. Electroanal. Chem. Interfacial Electrochem.*, 1972, **38**, 25–43.
- 21 E. Frackowiak and F. Béguin, *Carbon N. Y.*, 2001, **39**, 937–950.
- 22 A. G. Pandolfo and A. F. Hollenkamp, *J. Power Sources*, 2006, **157**, 11–27.

- 23 A. J. Bard and L. R. Faulkner, *Electrochemical methods - Fundamentals and Applications*, John Wiley & Sons, Inc, 2nd edn., 2001.
- 24 E. J. van der Wouden, E. A. Tolner, M. Odijk, W. Olthuis, A. M. J. M. van den Maagdenburg, M. D. Ferrari, and A. van den Berg, in *2013 Transducers & Eurosensors XXVII: The 17th International Conference on Solid-State Sensors, Actuators and Microsystems (TRANSDUCERS & EUROSensors XXVII)*, 2013, pp. 2145–2148.

SI-1: Details of the one-dimensional Comsol model for capacitive deionization.

Version: Comsol 4.4 (Build:195)

Global definitions

Variables

Table 1 Variables

Name	Expression	Description
Dcl	2.00E-09	m ² /s
Dna	2.00E-09	
Dh	9.30E-09	m ² /s
Doh	5.27E-09	
F	96485	C/mol
R	8.314	J/Kmol
T	298	K
Cna_init	2.00E-02	mol/m ³ or mM
Ccl_init	Cna_init	
Kw	1.00E-14	mol/m ³
V_elec	0.75	V
epsilon	78*8.854e-12	
uh	Dh*F/R/T	
uoh	Doh*F/R/T	
una	Dna*F/R/T	
ucl	Dcl*F/R/T	
lambda_S	3.00E-10	
t_rc	15*60	minutes

Applied waveform (rect1)

Lower limit: 2.75

Upper limit: t_rc+2.75

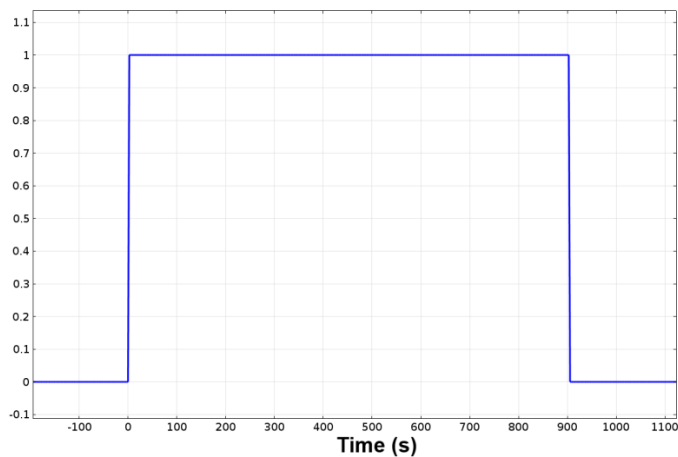


Figure 1 Rectangular function (rect1).

Model1 (mod1)

Definitions

The standard form of the Poisson's equation and PDE are used in the model. This means that Comsol does not know about any constraints concerning the finite amount of ions in the solution. To prevent the concentration to become less than zero a substitution is made:

Variables

$$Cna = \exp(qna)$$

$$Ccl = \exp(qcl)$$

Geometry1

Length unit: m

Angular unit: degrees

Default relative repair tolerance: 1E-6

Interval (i1)

Number of intervals: One

Left endpoint: 0 m

Right endpoint: 3.1E-3

Form union (fin)

Action: Form a union

Relative repair tolerance: 1E-6

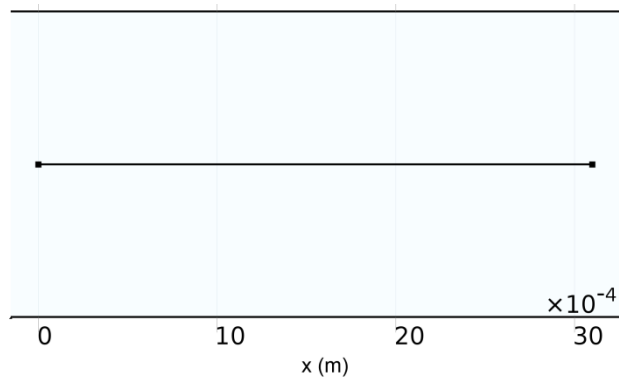


Figure 2 Geometry of the model. One dimensional with a length of 3.1mm.

Poisson's equation (poeq)

Dependent variable: V

$$\text{Poisson's Equation1: } \nabla \cdot (-c\nabla V) = f$$

$$c=1$$

$$f= F*(\exp(qna)-\exp(qcl))/\epsilon$$

Initial values:

$$V = 0$$

$$\frac{\partial V}{\partial t} = 0$$

$$\text{Flux/Source1: } -n \cdot (-c\nabla V) = g - qV$$

$$g= -0.5*V_elec*(\text{rect1}(t))/\lambda_S$$

$$q= 1/\lambda_S$$

Flux/Source2: $-n \cdot (-c\nabla V) = g - qV$
 $g = 0.5 * V_{elec} * (rect1(t)) / \lambda_{S}$
 $q = 1 / \lambda_{S}$

PDE(g) / Nernst-Planck (diffusion and migration)

Dependent variables: qna, qcl

General form PDE1: $e_a \frac{\partial^2 u}{\partial t^2} + d_a \frac{\partial u}{\partial t} + \nabla \cdot \Gamma = f$

$\Gamma =$
 $-\exp(qna) * (Dna * qnax + una * Vx)$
 $-\exp(qcl) * (Dcl * qclx - ucl * Vx)$

$f =$
 0
 0

$d_a =$

$\exp(qna)$	0
0	$\exp(qcl)$

$e_a =$

0	0
0	0

Zero Flux1: $-n \cdot \Gamma = 0$

All boundaries

Initial Values1:

$qna = \log(Cna_init)$

$qcl = \log(Ccl_init)$

$\frac{\partial qna}{\partial t} = 0$

$\frac{\partial qcl}{\partial t} = 0$

Mesh1

User controlled mesh

Size:

Calibrate for general physics (custom)

Maximum element size = 1E-4

Maximum element growth rate = 1.1

Resolution of narrow regions = 1

Distribution:

Predefined distribution type

Number of elements = 1500

Element ratio = 1500

Distributed method: Geometric sequence (symmetric distribution)

Edge1

Domain: All domains

Study1

Step 1: Time Dependent

Time unit = s

Times = range(0,(2*t_rc-0)/3999,2*t_rc)

Relative tolerance = 1E-3

Solver Configurations

Solver1

Time-Dependent Solver1

Time stepping method = BDF

Steps taken by solver = Free

Initial step = 1E-10s

Max./Min. BDF order = 1

Event tolerance = 0.01

SI-2 Schematic of the battery powered voltage source.

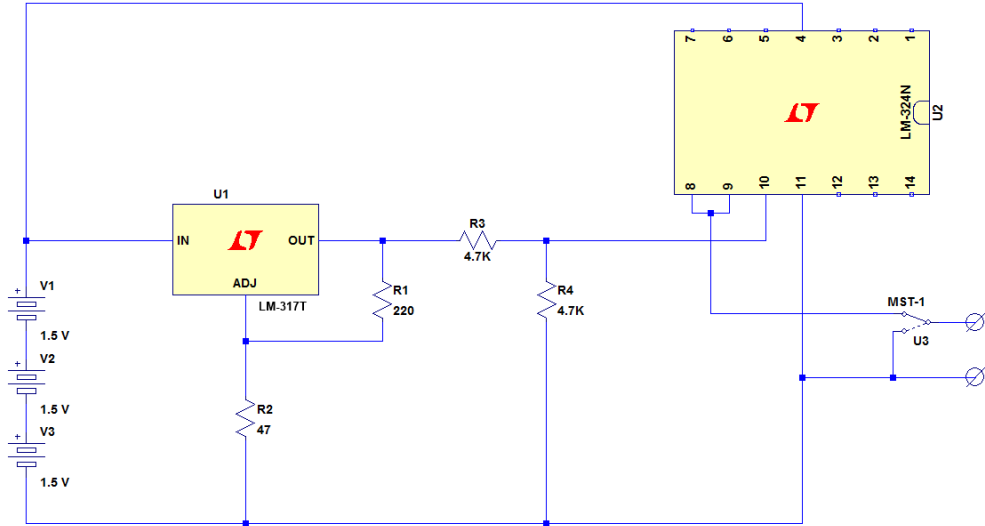


Figure 1 Diagram of the battery powered voltage source.

Table 1 Bill of Materials

Component	Description/Value
R1	resistor, 220, 5%
R2	resistor, 47, 5%
R3	resistor, 4.7K, 5%
R4	resistor, 4.7K, 5%
U1	LM-317T
U2	LM-324N
U3	MST-1

SI-3: Overview EIS measurements for different ion concentrations.

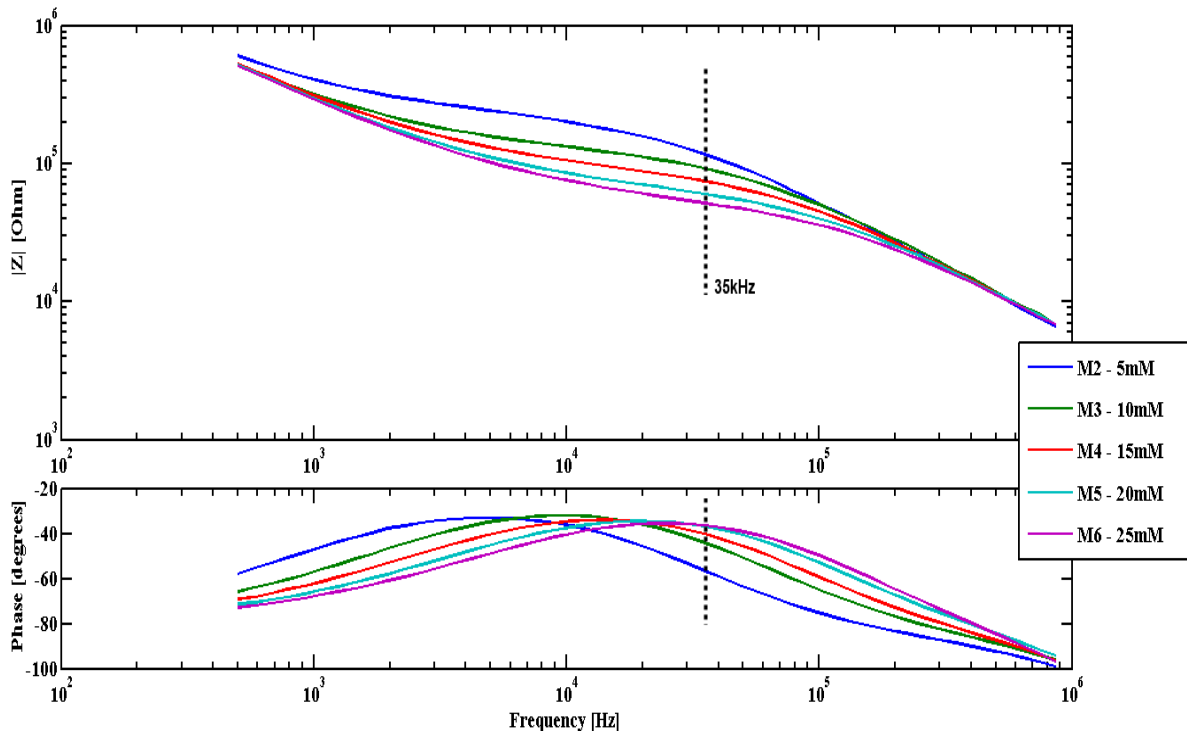


Figure 1 Bode plot for five NaCl solutions with different concentration. The dashed line depicts the measurement frequency at 35kHz.

Bode plots have been created using the in-house developed lock-in amplifier. The impedance is measured between 500Hz and 1MHz in 50 logarithmically divided steps. For every concentration, five measurements have been averaged. The results are shown in Figure 1.

In the impedance plot, three distinct regions can be seen. The first is a steady decline characterized by the double layer capacity.

The second part is the (almost) horizontal plateau. This is called the resistive plateau, where only the resistivity contributes to the impedance. Ideally, when it is a pure resistance, the phase will become zero. In this case, the maximum phase reaches $\sim 30\text{deg}$.

The last region is again a steady decline. This decline is due to parasitic capacities.

The frequency, at which the transitions between the regions occur, is dependent on the resistivity and the capacities. As the capacities are nearly constant, these transition points shift with the change in resistivity. The resistivity is linearly dependent on the concentration ions. That is why in Figure 1 the line shifts downwards and to the right with increasing concentration.

The frequency at which the EIS measurements were done was 35kHz. This frequency has been depicted in Figure 1 by a dashed line. When looked at 25mM and 20mM the measurement would be in the resistive plateau. When 5mM is considered however, the measurement would be done in the region where the parasitic capacities contribute to the impedance.

This means that the lower the concentration becomes, the more the measured impedance will be dominated by the parasitic capacity. The measured impedance will therefore be lower than the resistivity of the solution. While the resistivity is linearly dependent on the concentration, the impedance is not.

Acknowledgements

First, I would like to thank the BIOS group as a whole. Over time during my study, I have been in contact with the BIOS group for several times. It started with Wouter Olthuis being the one explaining me how electric fields work back in 2001. This was followed by a D2 project in I believe 2002. The group has been a great influence on my choice to pursue the master specialization Biomedical Systems. I ended up doing multiple courses given by this group and eventually did my bachelor and master thesis here. What amazes me the most about this group, is that although the group expended a lot, changed venue and many members have come and gone, the social dynamic has pretty much stayed the same. I hope the group can keep this up as to me, this is a very nice working environment.

In special, I would like to thank Susan. She has been my daily supervisor with my bachelor assignment and with my master thesis. With a different study background your insights where most of the times very different from mine, giving me the opportunity to look at things in another way than my electrical engineering way.

Furthermore, I would like to thank Mathieu. Although he was on paper not my daily supervisor, he has been for the last months due to the maternity leave of Susan. When we are honest, due to your interest in the project you might as well have been a daily supervisor on paper.

I would like to thank Jan for being my overall supervisor and James Seddon of the Nanoionics group for being willing to be part of my examination committee.

Due to back problems, my master thesis has taken a lot of time. I would like to compliment Susan, Mathieu and Jan in the way they have handled this situation and giving me the opportunity to continue with my work. I want to emphasize that it was much appreciated that I could continue my work under conditions necessary for my recovery and at my own pace.

Then it is time to thank my girlfriend Diewertje, for supporting me all this time and notching me in the right direction. This is a great achievement on her part, to be able to notch me by just the right amount so I would increase my efforts, without me being offended.

At last, I would like to thank my parents and sister for giving me the opportunity to study, even when it took so much time.